Stability and composition of CH_4-rich clathrate hydrates in the present martian subsurface

Elodie Gloesener[a,b,*], Özgür Karatekin[b], Véronique Dehant[a,b]

[a] *Earth and Life Institute, Université Catholique de Louvain, Louvain-la-Neuve, Belgium*
[b] *Royal Observatory of Belgium, Brussels, Belgium*

Abstract

In the past years, multiple detections of methane in Mars' atmosphere have raised numerous questions about its potential sources. Independently of methane formation mechanism(s), CH_4 produced in the past or at the present day could be stored in subsurface reservoirs such as clathrate hydrates. In this work, global maps of stability depth of CH_4-rich clathrate hydrates in the martian soil are obtained by including in the subsurface model a top layer with thermal properties that fit with the thermal inertia derived from MGS TES observations (Putzig and Mellon, 2007) and by taking into account the spatial variations of the surface heat flow (Parro et al., 2017). In addition, the spatial distribution of stable methane clathrates is investigated in the presence of eutectic NaCl and $CaCl_2$ brines. The influence of gas phase composition on clathrate stability and on guests abundance is also examined by considering the CO_2-CH_4-N_2 and CO_2-CH_4-H_2 mixtures.

On present-day Mars, the stability conditions of CH_4-rich clathrates are

*Corresponding author. Royal Observatory of Belgium, Avenue Circulaire 3, 1180 Brussels, Belgium. Tel.: +32 27 90 39 28.

Email address: elodie.gloesener@observatory.be (Elodie Gloesener)

met at a depth of a few meters in high latitude regions and at a few tens of meters deep at the equator. The top of their stability zone is the deepest (∼68 m) in regions where methane has been locally reported, especially in the area observed by Mumma et al. (2009). It is also in that particular region that the methane clathrate stability zone is the least extended in the martian subsurface, its base reaching ∼8 km deep in the presence of pure water. This depth can even be 4 times shallower if methane clathrates form in the presence of eutectic $CaCl_2$ brine. Moreover, the incorporation of nitrogen and hydrogen in mixed CO_2-CH_4 clathrates allows a better trapping of methane but their presence increases the formation pressure and therefore their stability depth.

Keywords:

Mars, Methane, Clathrate hydrates

---

1. Introduction

Several detections of methane (CH_4) in the martian atmosphere have been reported from Earth-based and Mars orbit instruments (Formisano et al., 2004; Krasnopolsky et al., 2004; Geminale et al., 2008, 2011; Mumma et al., 2009; Fonti and Marzo, 2010) with abundances ranging up to tens of parts per billion by volume (ppbv). Moreover, in situ measurements performed at Gale crater by the Curiosity rover showed some peaks up to $\sim$7 ppbv and an apparent seasonal cycle of the CH_4 background levels (Webster et al., 2015, 2018). However, more time series of methane abundance estimates would be necessary to confirm this periodic variation (Gillen et al., 2020). Recently, first measurements from the ExoMars Trace Gas Orbiter (TGO) mission, especially designed to look for trace levels of methane, did not show any CH_4 detection with an upper limit of about 0.05 ppbv (Korablev et al., 2019).

The only methane sink currently accepted on Mars is its photochemical destruction through its photolysis by the Lyman α line above $\sim$80 km altitude, and its oxidation by OH or $O(^1D)$ below (Haberle et al., 2017). This leads to a CH_4 chemical lifetime of about 300 terrestrial years (Lefèvre and Forget, 2009), much larger than both vertical and horizontal mixing times (10 days and 0.5 year respectively) (Krasnopolsky et al., 2004). Accordingly, methane was expected to be well-mixed in the martian atmosphere. Both remote-sensing and in situ observations have nonetheless evidenced substantial variations of the CH_4 mixing ratio implying an atmospheric lifetime of less than 200 days (Lefèvre and Forget, 2009) and suggesting the presence of localized release and fast removal processes. Methane variability on short time scales has raised numerous questions and the validity of CH_4 detections

have been debated (Zahnle et al., 2011; Villanueva et al., 2013; Zahnle, 2015; Webster et al., 2018) on the basis that methane retrievals were distorted due to improper corrections of telluric lines or that some residual terrestrial methane was present in the rover chamber. However, erroneous detections seem surprising given that unsuccessful searches for CH_4 on Mars have also been reported from ground-based (Mumma et al., 2009; Villanueva et al., 2013) and Curiosity (Webster et al., 2013) measurements.

Although an in situ spike detection has been recently confirmed from orbit by the Mars Express team who reanalyzed data recorded in 2013 (Giuranna et al., 2019), the existence of unknown and rapid destruction mechanisms is required to explain simultaneously the presence of intermittent CH_4 peaks at the surface and the TGO global non-detection. Several methane loss processes have been proposed such as heterogeneous chemistry (Lefèvre and Forget, 2009), triboelectricity (Farrell et al., 2006; Atreya et al., 2007) or physical and chemical sequestration in the soil (Gough et al., 2010; Jensen et al., 2014) but none of them has been identified to date.

The observed methane variability results from a competition between sinks and sources. It has been proposed that methane on Mars could originate from biological (Atreya et al., 2007; Weiss et al., 2000), geological (Oze and Sharma, 2005; Etiope and Sherwood Lollar, 2013) or exogenous (Kress and McKay, 2004; Keppler et al., 2012) generation mechanisms. On the other hand, CH_4 produced in the past or at the present day could be stored in subsurface reservoirs such as clathrate hydrates (Chastain and Chevrier, 2007) or zeolites (Holmes et al., 2015; Mousis et al., 2016). Clathrate hydrates, also called clathrates, are crystalline compounds constituted by cages formed by

hydrogen-bonded water molecules inside of which guest gas molecules are trapped. Thermodynamic conditions prevailing in the martian subsurface favor clathrate formation from 15 m down to 24 km deep (Max et al., 2011) and kinetic experiments (Gainey and Elwood Madden, 2012) showed that their dissociation, stimulated by pressure and temperature changes, is a feasible mechanism for near-surface methane release.

Clathrates are known for their capacity to store a large amount of gas. At standard pressure and temperature conditions, one cubic meter of CH_4 clathrates contains more than 160 cubic meters of methane and the dissociation of 2×10^3 m^3 of such a reservoir would be required each year to explain a steady-state value of 10 ppb in the martian atmosphere. Their actual presence depends on the availability of methane and water. Clathrate deposits could therefore be very localized and occupy only a small part of the martian cryosphere, which would be consistent with the observed spatial heterogeneity of methane. Near-surface reservoirs could episodically discharge methane in the atmosphere following destabilizing events such as impacts, climatic changes or faults and landslides generated by seismicity. On the other hand, one can suggest the formation of clathrates on the south permanent polar cap as a potential methane sink. However, this loss mechanism has been showed not to play a significant role in the dynamics of atmospheric methane on present-day Mars (Thomas et al., 2009; Herri and Chassefière, 2012).

The clathrate global distribution on Mars is expected to be at least as complex as on Earth (Lasue et al., 2015). The formation/dissociation cycle of clathrates and the thickness of their stability zone depend on many factors such as subsurface composition, local heat flow, salinity of the water involved

in their formation (Elwood Madden et al., 2007) and climate change due to seasonal and obliquity variations (Prieto-Ballesteros et al., 2006; Root and Elwood Madden, 2012). This work results from the need to provide a better estimation of the subsurface distribution of clathrates on Mars in order to constrain depth of possible source(s) of methane. We thus define in the following an upper bound to possible clathrate occurrences by determining global stability regions based on temperature-pressure conditions. Moreover, clathrate hydrates on Mars might be exposed to highly concentrated salt environments. Although its effects on the formation and stability of clathrates are not well understood, salinity is an important factor to take into account as it depresses the freezing point of water and thus influences the temperature at which clathrates form and dissociate.

In the first part of this paper, a sensitivity study is performed to determine variations of methane clathrate stability zone (CSZ) as a function of thermal properties of the subsurface and heat flow. In the second part, global maps of stability depth of CH_4-rich clathrate hydrates in the martian soil are obtained for the first time by including in the subsurface model a top layer with thermal properties that fit with the thermal inertia derived from MGS TES observations (Putzig and Mellon, 2007). In addition, the spatial distribution of stable methane clathrates is investigated in the presence of eutectic NaCl and $CaCl_2$ brines. Finally, we examine the effect of gas phase composition on clathrate stability and on guests abundance by considering the CO_2-CH_4-N_2 and CO_2-CH_4-H_2 mixtures. The latter is examined since most of the methane generation mechanisms imply H_2 production.

2. Clathrate hydrate stability zone model

2.1. Clathrate hydrate model

We follow an approach similar to Thomas et al. (2009) where the dissociation pressure P_{mix}^{diss} of a multiple guest clathrate is calculated from the dissociation pressures of simple guest clathrates as (Lipenkov and Istomin, 2001):

$$P_{mix}^{diss} = \left(\sum_{G} \frac{x_G}{P_G^{diss}} \right)^{-1} \tag{1}$$

where x_G is the molar fraction of species G in the initial gas phase. The dissociation pressure P_G^{diss} of a simple clathrate of guest species G follows an Arrhenius law (Miller, 1961):

$$\log(P_G^{diss}) = A + \frac{B}{T} \tag{2}$$

where P_G^{diss} is expressed in Pa and T is the temperature in K. The constants A and B fit to experimental data (Deaton and Frost, 1946; Larson, 1955; Marshall et al., 1964; Jhaveri and Robinson, 1965; Takenouchi and Kennedy, 1965; Robinson et al., 1967; Miller and Smythe, 1970; Falabella, 1975; Holder et al., 1980; Ng and Robinson, 1985; Makogon and Sloan, 1994; Kuhs et al., 2000; Yasuda and Ohmura, 2008; Mohammadi and Richon, 2010, 2011; Chapoy et al., 2010) and are listed in Table 1 with the temperature range in which they are valid.

When thermodynamic inhibitors such as salts are present in the system, they change the activity of water which affects both the freezing point of pure water and the clathrate stability conditions. As a consequence, when

Table 1: Parameters A and B (K) required in Eq.(2).

Molecule	A	B (K)	T range (K)
CH_4	9.65	-895.9	$\leq$ 272.9
CH_4	21.46	-4124.4	$\geq$ 272.9
CO_2	10.13	-1116.9	$\leq$ 273.1
N_2	9.74	-702.57	$\leq$ 271.9
Ar	9.24	-630.86	$\leq$ 272.2
H_2	19.70	-3080.7	$\geq$ 263.85

salinity increases in the free water phase resulting in a decrease of the ice - liquid water transition, it moves the quadruple point (where ice, liquid water, clathrate and gaseous phases coexist) towards lower temperatures with a shift that depends on the inhibitor concentration. The dissociation curve of clathrate hydrates is thus shifted approximately parallel to the uninhibited phase boundary (on a plot of ln P versus T) towards lower temperature and higher pressure (Sloan and Koh, 2007). The dissociation pressure corresponding to temperature larger than the eutectic temperature has been estimated assuming slopes comparable to the pure water system, similarly to the approach of Elwood Madden et al. (2007) for systems with eutectic NaCl and $CaCl_2$ brines.

Once the equilibrium pressure is known, the relative abundance of a species G in a clathrate hydrate is given by:

$$x_G^H = \frac{b_s \theta_{G,s} + b_l \theta_{G,l}}{b_s \sum_J \theta_{J,s} + b_l \sum_J \theta_{J,l}} \tag{3}$$

where the sum at the denominator takes into account all the species in the gas phase and b_s and b_l are the number of small and large cavities per unit cell respectively. The occupancy fraction θ is calculated following the model of van der Waals and Platteeuw (1959) described in Appendix A.

2.2. Subsurface model

A one dimensional thermal diffusion equation for subsurface temperature with depth dependent thermal conductivity, density and specific heat is solved with a Crank-Nicolson scheme on a grid with variable spacing:

$$\rho(z)c(z)\frac{\partial T(z,t)}{\partial t} = \frac{\partial}{\partial z}\left(k(z)\frac{\partial T(z,t)}{\partial z}\right) + \rho(z)H \tag{4}$$

where ρ is density, c is specific heat capacity, T is temperature, z is vertical coordinate, t is time, k is thermal conductivity and H is radiogenic heat production. The latter has only a modest effect for temperature determination and is set to a constant value (5×10^{-11} W kg^{-1}) assuming a vertically homogeneous distribution of radiogenic heat-producing elements in the planet's crust (Hahn et al., 2011).

In our simulations to determine global maps of the clathrate stability zone, the changes in surface temperature and pressure in latitude and longitude over the martian year are given by the Mars Climate Database v5.2 ("Climatology" scenario, average solar EUV conditions) (Forget et al., 1999; Millour et al., 2015). The present-day heat flow variations across the martian surface are taken from the model of Parro et al. (2017) that provides a surface heat flow varying between 14 and 25 mW m^{-2} with an average value of 19 mW m^{-2} and the subsurface model is divided in two layers. The thermal properties of the upper layer are set to fit with the thermal inertia derived from Mars Global Surveyor Thermal Emission Spectrometer observations (Putzig and Mellon, 2007). Accordingly, the regolith bulk density ρ_b (kg m^{-3}) of this layer is determined as a function of thermal inertia I (J m^{-2} K^{-1} s$^{-1/2}$) following the empirical relation from Mellon and Jakosky (1993):

$$\rho_b = 150 + 100\sqrt{34.2 + 0.714I} \tag{5}$$

with a maximum value assumed to be 2500 kg m^{-3}. The specific heat capacity c is set to 800 J kg^{-1} K^{-1} and the thermal conductivity k is then determined using $k = I^2/(\rho_b c)$. The properties of the lower layer depend on the latitude of the studied area. Between 50°N and 50°S, the top of the lower layer is set to 1 m deep and its thermal properties are representative of dry basalt. Northward of 50°N and southward of 50°S, the lower layer starts at 50 cm deep and has thermal properties representative of ice-saturated soil. This choice is based on the subsurface water ice stability predicted by equilibrium models (Mellon et al., 2004; Schorghofer and Aharonson, 2005). The compression of pore spaces with depth is modelled following Clifford (1993):

$$\Phi(z) = \Phi_0 \exp(-z/K_0) \tag{6}$$

where Φ_0 is the surface porosity (40%), z is the depth and K_0 is the porosity decay constant ($\sim$ 2.82 km). The variations of the volumetric heat capacity and thermal conductivity with depth are then given by:

$$\rho c(z) = (1 - \Phi(z))\rho_{\rm dry} c_{\rm dry} + \Phi(z)\rho_{\rm ice} c_{\rm ice} \tag{7}$$

$$k(z) = k_{\rm dry}^{(1-\Phi(z))} k_{\rm ice}^{(\Phi(z))} \tag{8}$$

where properties of water ice and basalt are referred in Table 2.

As mentioned above, we consider a basaltic mineralogy for the second layer of our subsurface model, either in the presence of water ice or not. However, local variations in the soil material could strongly affect the methane

Table 2: Typical thermophysical properties of geological materials used in this study.

	k (W m^{-1} K^{-1})	ρ (kg m^{-3})	c (J kg^{-1} K^{-1})	I (J m^{-2} K^{-1} s$^{-1/2}$)
Water ice	2.8	920	1960	2247
Basalt	2	3000	800	2190
Ice-saturated soil	2.5	2018	1040	2290
Dry unconsolidated soil	0.045	1650	800	244

clathrate distribution in the martian subsurface. Therefore, in the following section, a sensitivity study is firstly performed to evaluate the impact of the soil properties, among others, on the stability field of clathrates. The latter is determined using different thermal properties in our subsurface model corresponding to thermal inertia ranging from 250 to 2000 J m^{-2} K^{-1} s$^{-1/2}$. For these simulations, the volumetric heat capacity ρc is kept constant (1.6 $\times$ 10^6 J K^{-1} m^{-3}) while the thermal conductivity k is changed accordingly.

The pressure in pore spaces that controls stability of methane clathrate hydrates in subsurface has two limiting cases: lithostatic pressure when the pore spaces are closed and atmospheric pressure when they are open (Schuerger et al., 2013). Clathrates need to be sealed off from the martian atmosphere to remain stable, except for a very limited region corresponding to the south polar cap where surface temperatures are cold enough to enable CO_2 clathrate formation (Mousis et al., 2013). If the subsurface pressure profile is determined assuming open porosity, pressure in pore spaces is thus too low to meet the CH_4-rich clathrate stability conditions at any depth and latitude. Accordingly, all results presented in this work have been calculated assuming a lithostatic pressure related to isolated porosity.

3. Results

3.1. Methane clathrate hydrate stability zone: a sensitivity study

In this sensitivity study, unless otherwise is stated, the stability depths are calculated based on the present-day mean annual surface temperatures (Clifford and Parker, 2001) while the surface heat flow and the surface pressure are constant and assumed equal to their average value, 19 mW m^{-2} (Parro et al., 2017) and 610 Pa respectively. The clathrate stability zone changes with seasonal variations will be addressed in the following section.

Regarding the subsurface composition, the type of soil directly controls the geothermal conditions and therefore the depth of clathrate formation. In Fig. 1, methane clathrate stability zone is determined in materials ranging from ice-cemented soil (A) to dry unconsolidated soil (D).

Similarly to previous studies (Chastain and Chevrier, 2007; Root and Elwood Madden, 2012), methane clathrate hydrates are expected to form at shallower depth with increasing latitude and their stability zone is thicker at high latitude. The thermal conductivity of the soil is a key parameter in the determination of the clathrate stability zone. Materials with high thermal conductivity such as sandstone or ice-cemented soil evacuate heat more efficiently and thus maintain lower temperatures, which allows clathrate formation with a stability zone of several kilometers thick. In Fig. 1A, CH_4 clathrate stability zone extends from about 45 m deep to 11.8 km deep at the equator and from 0.6 m deep to about 22 km deep at the pole. On the contrary, if thermal conductivity is not high enough to maintain the low temperature required for clathrate formation, clathrate stability conditions are never met in equatorial regions or only on a small subterranean layer a

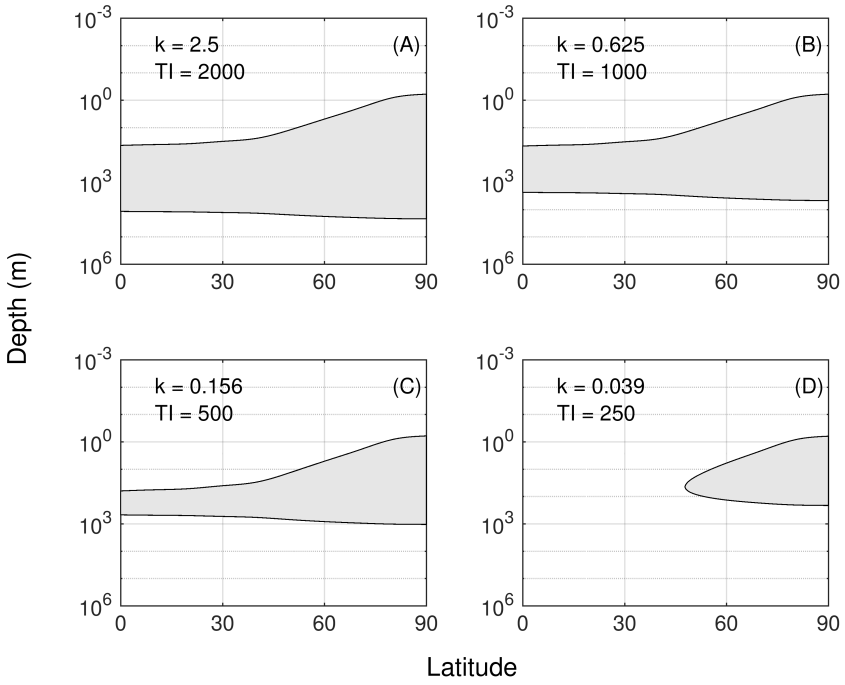

Figure 1: Stability zone of simple CH_4 clathrate in the martian crust for different thermal properties in the subsurface model corresponding to thermal inertia (TI) ranging from 250 to 2000 J m^{-2} K^{-1} s$^{-1/2}$. The volumetric heat capacity ρc is kept constant (1.6 $\times$ 10^6 J K^{-1} m^{-3}) while the thermal conductivity k is changed to 2.5 (A), 0.625 (B), 0.156 (C) and 0.039 W m^{-1} K^{-1} (D) respectively.

few hundred meters thick as shown in Fig. 1.

The base of methane CSZ being located several kilometers deep in the martian subsurface, its variations in depth are highly affected by the local heat flow as shown in Fig. 2, where calculations have been made for an ice-cemented soil. As expected, the depth up to which the stability zone extends decreases with increasing heat flow. The methane clathrate stability zone

extends until 15 km deep at the equator when the heat flow is 14 mW m^{-2}, while its base is 2 times shallower with a heat flow of 25 mW m^{-2}. This behavior has significant implications for clathrate formation on Early Mars where surface heat flows were quite high compared to present-day values.

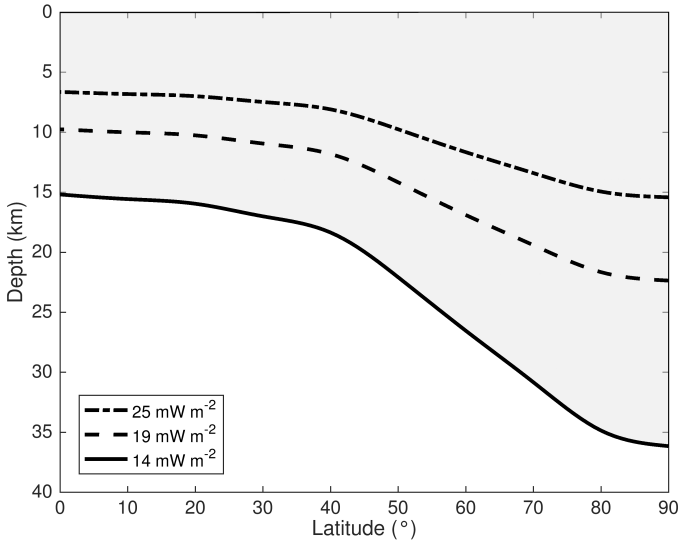

Figure 2: Depth of the base of methane clathrate stability zone as a function of latitude for different values of the heat flow (14, 19 and 25 mW m^{-2}).

3.2. Methane clathrate hydrate stability zone: global maps

Previously, the stability zone of methane clathrate hydrates in the martian subsurface has been determined using present-day mean annual surface temperatures. However, oscillations of temperature due to seasonal variations can propagate over several meters deep and so reach the clathrate stability zone at locations where it is close to the surface. Consequently, at high latitude, the shallow stability zone will be shifted downwards during

warm seasons when the soil temperatures are too high to maintain stable clathrates and inversely during the colder time periods. The depth at which temperature fluctuation is reduced by 63% (and thus equals 1/e (∼0.37) of the surface temperature oscillation) is given by the skin depth δ:

$$\delta = \sqrt{\frac{kP}{\rho c \pi}} \tag{9}$$

where P is the time period of variations (for seasonal changes, $P = 1$ martian year). With thermal properties similar to those of Fig. 1A, $\delta = 5.4$ m. At latitudes higher than 60°, the methane clathrate stability zone is shallower than this annual skin depth and will therefore be influenced by seasonal variations. For Fig. 1C, δ is 3 times smaller, which makes the seasonal changes in the clathrate stability zone significant beyond a latitude of 75° in that case.

Here, fluctuations of the clathrate stability depth over a martian year are studied and global maps of the maximum depth reached by the top of the CSZ are obtained. The latter represents therefore the depth from which clathrate hydrates remain unaffected by seasonal cycles. For these simulations, the subsurface model extends to 100 m deep and mixed CO_2-CH_4-N_2-Ar clathrates are considered with ratios between CO_2, N_2 and Ar comparable to those measured on Mars. These mixed clathrates trapping the main components of the martian atmosphere together with methane are more representative of those that would presently form on the Red Planet compared to simple CH_4 clathrates studied in the previous section. Two CH_4 mole fractions in the initial gas phase forming clathrates are considered: 90%, which leads to the formation of CH_4-rich clathrates, and 1% resulting in CO_2-rich clathrates.

At first, in order to have an idea of the kind of variations experienced by the stability zone, we present in Fig. 3 the evolution over time of the top of the CSZ for clathrates formed from a gas phase with 90% of methane, at Phoenix landing site. At the beginning of the year, around a solar longitude (L_S) of 25°, the CSZ is the closest to the surface with a depth of ∼2 m. Then the top of the stability zone is shifted downwards with time due to increasing surface temperature and reaches its maximum depth (∼5 m) around L_S = 198°. Then, the top of the clathrate stability zone approaches again the surface due to the decrease of surface temperature.

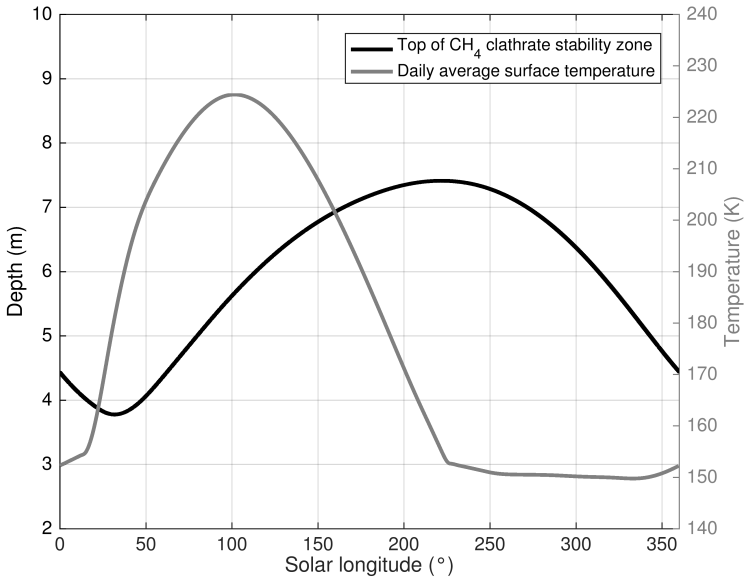

Figure 3: Variation over the year of the top of methane CSZ in the subsurface for clathrates formed from a gas phase with 90% CH_4 and daily average surface temperature at Phoenix landing site. Temperature variation is taken from MCD5.2.

The depth from which CH_4-rich clathrates remain unaffected by sea-

sonal variations in surface temperature within the martian subsurface at the present day is represented in Fig. 4. The top of the CSZ has been calculated, following the model described in section 2, every 5 degrees and then interpolated every degree. Local detections of methane are reported in black: Gale Crater (Webster et al., 2015, 2018) is represented as a black star, while Syrtis Major, Terra Sabae and Nili Fossae (Mumma et al., 2009) are included in the black rectangle.

At the present day, as stability conditions of methane clathrates are met in the near subsurface of Mars, the spatial variation of the top of their stability zone is strongly dependent on mean annual surface temperature. Consequently, CH_4-rich clathrate hydrates are stable closer to the surface at high latitude (few meters deep) and deeper in equatorial areas (few tens of meters deep) due to the larger surface temperature in these regions. By taking into account the thermal inertia observed by MGS TES (Putzig and Mellon, 2007) to set the thermal properties of the upper layer in our subsurface model and then increasing the thermal conductivity of the second layer to correspond to dry basalt, we found that the stability zone of CH_4-rich clathrates is the deepest in regions where methane has been locally reported, especially in the area observed by Mumma et al. (2009) where it is located $\sim$68 m deep and it extends over several kilometers in the martian subsurface. At this depth, clathrates can not be affected by seasonal changes in temperature. However, the addition of CO_2 in CH_4 clathrate hydrates decreases the dissociation pressure in the same temperature conditions, allowing them to be stable at shallower depths (Chastain and Chevrier, 2007). The spatial variation of the top of the CSZ for clathrates formed from a gas phase containing 1% CH_4

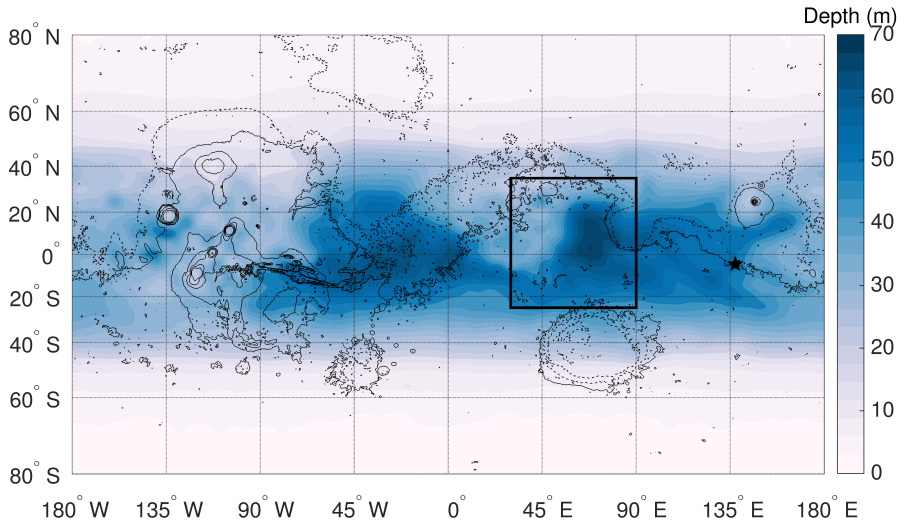

Figure 4: Depth (m) of the top of the clathrate stability zone in present-day martian subsurface for CH_4-rich clathrates formed from a gas phase with 90% of methane. The first layer of the thermal model has properties that fit with the thermal inertia derived from MGS TES observations (Putzig and Mellon, 2007), while the second layer has properties representative of dry basalt or ice-cemented soil depending on the latitude. Local detections of methane are reported in black: Gale Crater (Webster et al., 2015, 2018) is represented as a black star, while Syrtis Major, Terra Sabae and Nili Fossae (Mumma et al., 2009) are included in the black rectangle.

(the main component is therefore CO_2) is shown in Fig. 5. We observe the same pattern as in Fig. 4 but the stability field is closer to the surface, the largest stability depth being 28 m. Note that if the thermal properties of the martian soil are kept identical to those derived from TES MGS observations in the second layer of the subsurface model, the conditions for CH_4-rich clathrate stability are never met between 50°N and 50°S, as it can be deduced

from Fig. 1D.

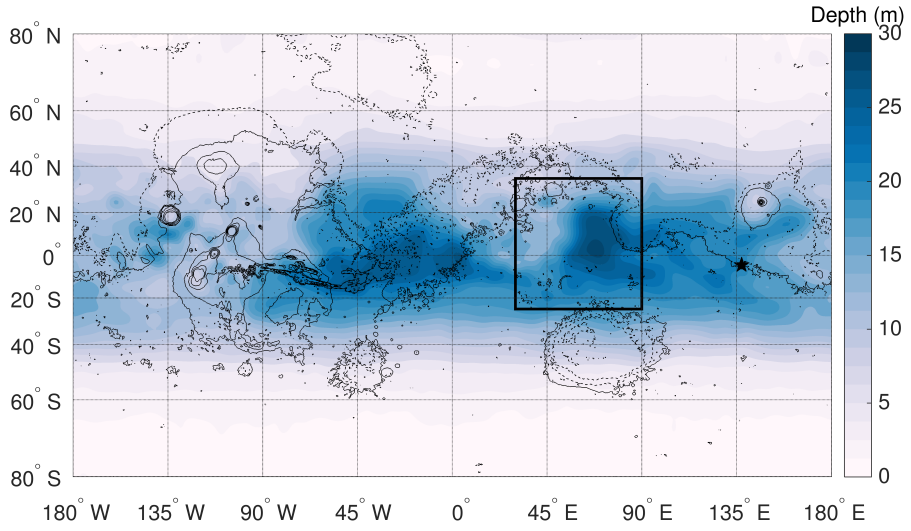

Figure 5: Same as Fig. 4 but for clathrates formed from a gas phase with 1% of methane.

As mentioned earlier, the presence of salts moves the stability curve of methane clathrate to lower temperature and higher pressure. This induces an upward shift of the base of the clathrate stability zone, which is therefore significantly narrowed (Elwood Madden et al., 2007). Here, we evaluate this shift across the martian surface by generating global maps for the base of the methane CSZ in the presence of eutectic NaCl and $CaCl_2$ brines. Results, presented in Fig. 6, show that the stability field of methane clathrate in the crust of Mars extends down to 8-12 km in equatorial regions and 14-21 km in high latitude regions in the presence of pure water. The base of the CSZ is strongly affected by the heat flow, as discussed in the previous section,

and is therefore deeper in the northern hemisphere and the Hellas Planitia region. Interestingly, it is closest to the surface in regions where methane was reported during the northern summer 2003 (Mumma et al., 2009). In the presence of eutectic NaCl and $CaCl_2$ brines, the base of the methane CSZ gets closer to the martian surface and reaches depths of 6-17 km and 2-13 km respectively, shallowest depths corresponding to the region including Syrtis Major and Terra Sabae.

3.3. Variability of methane trapping

Methane currently generated at depth in the martian crust would migrate upwards to reach the local clathrate stability zone and be enclathrated. The trapping of the different species present in the initial gas phase depends on the interactions between the guest molecules and the clathrate cages, as well as the partial pressures of the gases present during and after formation. Fig. 7 shows the fraction of methane in mixed CO_2-CH_4-N_2-Ar clathrates as a function of the CH_4 initial abundance in the gas phase for structures I and II. In the presence of CO_2, the formation of CH_4-rich clathrate hydrates is possible only if the initial gas phase is enriched in methane (Thomas et al., 2009). Moreover, methane trapping is slightly enhanced when formation temperature increases. At 270 K, to form clathrates trapping 50 % of methane in their cavities, the initial gas phase must contain about 68 % CH_4 and 57 % CH_4 for structures I and II respectively.

Here, we investigate the effect of gas phase composition on clathrate stability and on guests abundance by considering the CO_2-CH_4-N_2 and CO_2-CH_4-H_2 mixtures. The CH_4 production mechanisms often involve H_2 which can be made available locally via serpentinization, while a gas phase enriched

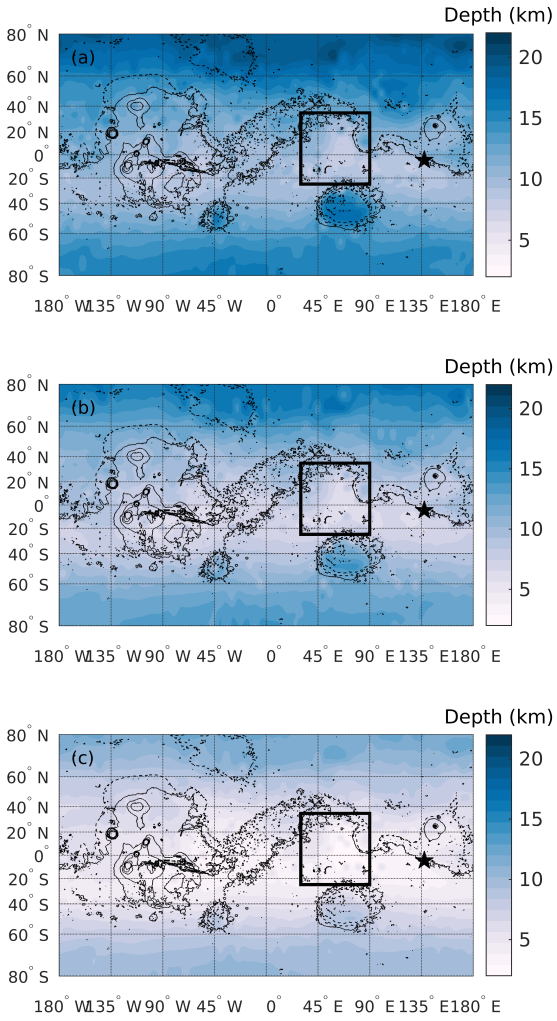

Figure 6: Estimated depth to the base of the clathrate stability zone for methane clathrate in the presence of pure water (a), eutectic NaCl brine (b), and eutectic $CaCl_2$ brine (c).

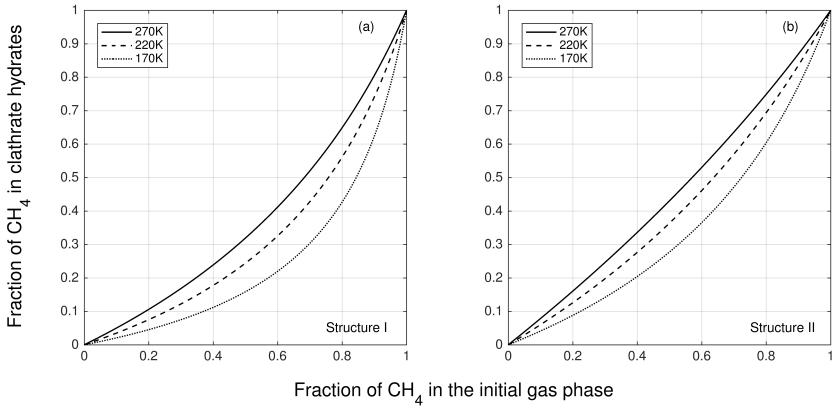

Figure 7: Fraction of CH_4 incorporated in mixed CO_2-CH_4-N_2-Ar clathrate hydrates as a function of the CH_4 fraction in the initial gas phase for different temperatures. The ratios between CO_2, N_2 and Ar are similar to those measured in the present martian atmosphere. Calculations have been made at the dissociation pressure of clathrates.

in N_2 is thought to be more representative of Early Mars atmosphere. Fig. 8 to 9 represent the formation pressure and the evolution of guests abundance, as a function of CH_4 mole fraction in the gas phase, in binary CO_2-CH_4 and ternary CO_2-CH_4-N_2 and CO_2-CH_4-H_2 sI clathrates at 270 K, respectively. The ratio between CO_2 and N_2/H_2 in the system is assumed to be 1. Although this ratio is probably unrealistic, the purpose here is to highlight the general trend for methane trapping in clathrates formed from a gas phase enriched in hydrogen or nitrogen. Firstly, it can be seen that the incorporation of nitrogen or hydrogen in mixed CO_2-CH_4 clathrates increases the formation pressure. For low CH_4 fraction (<0.1) in the gaseous phase, the formation pressure is multiplied by about 1.9 and 2 due to the presence of N_2 and H_2 respectively. It can also be seen that nitrogen and hydrogen are weakly

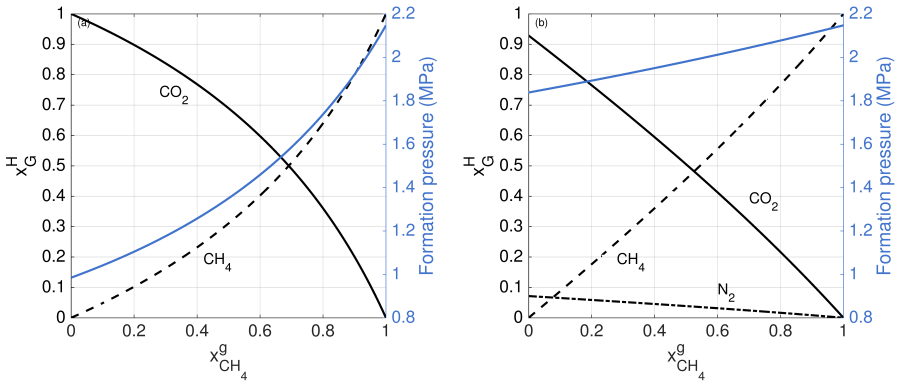

Figure 8: Formation pressure and fraction of the different guests x_G^H in (a) binary CO_2-CH_4 and (b) ternary CO_2-CH_4-N_2 sI clathrates at 270 K and as a function of CH_4 mole fraction in the gas phase. The ratio between CO_2 and N_2 in the gas phase is assumed to be 1.

trapped in mixed CO_2-CH_4 sI clathrates, their maximum relative abundance reaching 0.07 and 3.45 10^{-3}, respectively, when no methane is present in the gas phase. However, their incorporation in clathrate hydrates allows a slightly better trapping of methane. For example, in Fig. 9, CO_2-CH_4-H_2 sI clathrates trapping 50% of methane in their cavities are formed from a gas phase consisting of 53% CH_4, while 69% are required without the presence of H_2. In addition, if the structure II is the one that crystallizes, clathrate will trap a greater fraction of methane, similarly to what is observed in Fig. 7.

4. Discussion and conclusions

If they exist, methane clathrates on Mars could provide a viable source of sporadic releases as their stability conditions are currently met in the shallow subsurface. These crystalline compounds can be stable very near the surface

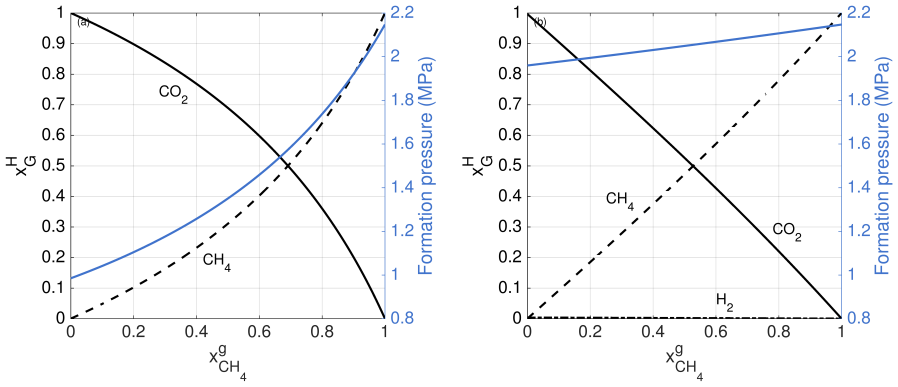

Figure 9: Formation pressure and fraction of the different guests x_G^H in (a) binary CO_2-CH_4 and (b) ternary CO_2-CH_4-H_2 sI clathrates at 270 K and as a function of CH_4 mole fraction in the gas phase. The ratio between CO_2 and H_2 in the gas phase is assumed to be 1.

at high latitudes, and can be as close as 20 m to the surface in the tropics. However, the top of their stability zone is the deepest (∼68 m) in regions where methane has been locally reported, especially in the area observed by Mumma et al. (2009). This depth is too great for clathrates to decompose due to seasonal changes in temperature. However, destabilizing events, such as seismic activity or impacts (Mousis et al., 2013), could dissociate clathrates locally and sporadically in agreement with methane observations. Indeed, these processes could release overburden pressure, increase local soil temperatures or open cracks and fractures that would therefore connect the clathrate reservoir to the surface leading to its destabilization and the methane release in the atmosphere.

Regarding the base of the methane clathrate stability zone on Mars, we showed that it is the shallowest (∼8 km) where Mumma et al. (2009) reported

observations of local methane plumes. In addition, when methane clathrates form in the presence of eutectic NaCl and $CaCl_2$ brines, the base of the stability zone gets closer to the martian surface, reaching in that particular region a depth of 6 km and 2 km respectively. The clathrate decomposition could be triggered at the base of the CSZ by interactions with high salinity fluids (Elwood Madden et al., 2007). In regions where CH_4 plumes have been observed, methane released by those deep clathrates would thus be transported through the crust along a shorter pathway to be either trapped again in subsurface reservoirs or discharged in the martian atmosphere.

As shown in section 3, the clathrate stability zone strongly depends on the heat flow values. If the methane production has stopped early in the martian history when surface heat flows were quite high, then formation of CH_4 clathrate reservoirs would have been limited to the stability zone associated to this time period. Thereafter, although the stability field of methane clathrate would have continued to expand with the cooling of the planet, new clathrate formations would not have occurred without the addition of methane in the system. Future studies specifically taking into account the thermal evolution of Mars would thus be required to further constrain depths of ancient clathrate reservoirs.

The formation of CH_4-rich clathrate hydrates from a gas phase containing carbon dioxide requires an initial gas phase enriched in methane. If those mixed CO_2-CH_4 clathrates form in contact with a significant fraction of nitrogen, as it may have been the case on Early Mars, or hydrogen, for example related to methane generation mechanisms, they can trap a larger amount of methane in their water cavities compared to clathrates formed

399 from carbon dioxide and methane exclusively. However, although N_2 and H_2
400 are weakly enclathrated, their presence strongly increases the formation pres-
401 sure of clathrate hydrates and therefore their stability depth. These ternary
402 clathrate hydrates trapping methane, if present in the near subsurface, would
403 be located deeper than binary CO_2-CH_4 clathrates. Their destabilization by
404 surface processes is therefore more challenging.

405 As shown in our sensitivity study, the clathrate stability zone is very re-
406 sponsive to the composition of the subsurface material. In our simulations
407 to establish global maps of the clathrate stability zone, we mainly consid-
408 ered a basaltic composition, which is fairly representative of the martian
409 crust. However, local variations in the soil material could strongly affect the
410 methane clathrate distribution displayed on our global maps and even pre-
411 vent clathrate formation at low latitude if the thermal conductivity of the
412 material is quite small. In order to further constrain the clathrate stability
413 field on Mars, geological observations coupled to a comprehensive sensitiv-
414 ity analysis with respect to soil parameters is thus required. In addition, our
415 global maps do not show metastable zones. Indeed, some clathrate reservoirs
416 could be localized outside their present stability field in areas associated to
417 ancient stability zones. These reservoirs could represent essential sources in
418 the study of methane outgassing scenarios since, being unstable, they would
419 gradually release methane from depths possibly very close to the surface. Ex-
420 perimental work on kinetic of clathrate formation and dissociation should be
421 used together with a subsurface thermal model taking into account obliquity
422 variations to evaluate the potential extent and locations of these metastable
423 clathrate reservoirs. Finally, in order to give a better accurate estimation of

the methane clathrate occurrences on Mars, a physical model such as the one presented in this work need to be coupled with topography/geological analysis to determine possible regions within the clathrate stability zone where sufficient CH_4 supplies could exist.

Appendix A. Thermodynamic modelling of clathrates

Thermodynamic equilibrium implies the minimization of the Gibbs energy and the equality of chemical potentials of water μ_w in the ice phase α and in the clathrate hydrate phase H:

$$\mu_w^H = \mu_w^\alpha \tag{A.1}$$

For convenience, this equalization can be rewritten in terms of chemical potential differences by introducing a hypothetical phase β that corresponds to a clathrate with empty cavities:

$$\left.\begin{aligned} \Delta\mu_w^{\beta-H} &= \mu_w^\beta - \mu_w^H \\ \Delta\mu_w^{\beta-\alpha} &= \mu_w^\beta - \mu_w^\alpha \end{aligned}\right\} \rightarrow \Delta\mu_w^{\beta-H} = \Delta\mu_w^{\beta-\alpha} \tag{A.2}$$

where μ_w^β is the chemical potential of water in the empty clathrate. $\Delta\mu_w^{\beta-\alpha}$ is determined from classical thermodynamics, while $\Delta\mu_w^{\beta-H}$ is evaluated via statistical thermodynamics. Following the model of van der Waals and Platteeuw (1959), this term can be written as a function of the occupancy fraction $\theta_{G,i}$ of a species G in a given type i of cage (i = small or large) for a given type of clathrate structure (I or II) as:

$$\Delta\mu_w^{\beta-H} = -RT\sum_i \nu_i \ln(1 - \sum_G \theta_{G,i}) \tag{A.3}$$

where R is the universal gas constant, T is the thermodynamic temperature and ν_i is the number of cavities of type i per water molecule in the clathrate unit cell. The occupancy fraction is defined as:

$$\theta_{G,i} = \frac{C_{G,i}(T) f_G(T,P)}{1 + \sum_J C_{J,i}(T) f_J(T,P)} \tag{A.4}$$

where $f_G(T,P)$ is the fugacity of the guest G in the gas or liquid phase and is calculated using the Peng-Robinson equation of state. The Langmuir constant $C_{G,i}(T)$ characterizes the attractiveness of the cavity i for a species G. If the cavity is assumed to be perfectly spherical and the guest molecule can freely rotate in the cage, the Langmuir constant can be written as:

$$C_{G,i}(T) = \frac{4\pi}{k_B T} \int_0^{R_c} \exp\left(\frac{-w_{G,i}(r)}{k_B T}\right) r^2 dr \tag{A.5}$$

where k_B is the Boltzmann constant, R_c is the radius of the spherical cavity and $w_{G,i}(r)$ is the spherically averaged potential energy between the guest molecule and the cavity. This interaction potential is often described by the Kihara potential (McKoy and Sinanoğlu, 1963):

$$w_{G,i}(r) = 2z\epsilon \left[\frac{\sigma^{12}}{R_c^{11} r}\left(\delta^{10} + \frac{a}{R_c}\delta^{11}\right) - \frac{\sigma^6}{R_c^5 r}\left(\delta^4 + \frac{a}{R_c}\delta^5\right)\right] \tag{A.6}$$

with

$$\delta^N = \frac{1}{N}\left[\left(1 - \frac{r}{R_c} - \frac{a}{R_c}\right)^{-N} - \left(1 + \frac{r}{R_c} - \frac{a}{R_c}\right)^{-N}\right] \tag{A.7}$$

where z is the coordination number of the cavity. The parameters R_c and z are specific to the type of cage and the clathrate structure and are listed in

Table A.1 for sI and sII clathrates. The Kihara parameters ϵ, a and σ are specific to the guest molecule and are determined by a linear regression fitted to experimental data. The set of Kihara parameters used in the present work is given in Table A.2. These parameters have been optimized by Herri and Chassefière (2012) in a study where they fitted the model of van der Waals and Platteeuw (1959) to compare the deviation from experimental data of pure clathrate hydrates at temperatures relevant to Mars.

Table A.1: Clathrate hydrate structure parameters (Sloan and Koh, 2007).

	sI		**sII**	
Cavity type	Small	Large	Small	Large
Number of cages per unit cell	2	6	16	8
Average cavity radius[a](Å)	3.95	4.33	3.91	4.73
Coordination number[b]	20	24	20	28

[a] The cavity radius will change with temperature, pressure and guest composition.

[b] The number of water molecules per cavity.

Table A.2: Kihara parameters used in the present study. These parameters are derived from Herri and Chassefière (2012) for CH_4, CO_2, N_2 and Ar and from Strobel et al. (2009) for H_2.

Molecule	ϵ/k_B (K)	σ (Å)	a (Å)
CH_4	166.36	3.0500	0.3834
CO_2	178.21	2.8730	0.6805
N_2	133.13	3.0993	0.3526
Ar	174.14	2.9434	0.1840
H_2	80.424	3.07838	0.1973

Acknowledgement

This work was supported by the Fonds de la Recherche Scientifique - FNRS under Grant n°EOS-30442502 and by the Belgian Science Policy Of-

fice (BELSPO) through the ESA/PRODEX Program. It received funding from the European Unions Horizon 2020 Program (H2020-694 Compet-08-2014) under grant agreement UPWARDS-633127. We would like to thank Norm Sleep and the anonymous reviewer for their comments which helped to improve this manuscript.

References

Atreya, S.K., Mahaffy, P.R., Wong, A.S., 2007. Methane and related trace species on Mars: Origin, loss, implications for life, and habitability. Planetary and Space Science 55, 358–369.

Chapoy, A., Gholinezhad, J., Tohidi, B., 2010. Experimental clathrate dissociations for the hydrogen + water and hydrogen + tetrabutylammonium bromide + water systems. Journal of Chemical & Engineering Data 55, 5323–5327.

Chastain, B.K., Chevrier, V., 2007. Methane clathrate hydrates as a potential source for martian atmospheric methane. Planetary and Space Science 55, 1246–1256.

Clifford, S.M., 1993. A model for the hydrologic and climatic behavior of water on Mars. Journal of Geophysical Research: Planets 98, 10973–11016.

Clifford, S.M., Parker, T.J., 2001. The evolution of the Martian hydrosphere: Implications for the fate of a primordial ocean and the current state of the northern plains. Icarus 154, 40–79.

487 Deaton, W.M., Frost, E.M., 1946. Gas hydrates and their relation to the
488 operation of natural gas pipe lines. US Bureau of Mines Monograph 8,
489 1–101.

490 Elwood Madden, M., Ulrich, S.M., Onstott, T., Phelps, T.J., 2007. Salinity–
491 induced hydrate dissociation: A mechanism for recent CH_4 release on Mars.
492 Geophysical research letters 34.

493 Etiope, G., Sherwood Lollar, B., 2013. Abiotic methane on Earth. Reviews
494 of Geophysics 51, 276–299.

495 Falabella, B.J., 1975. A study of natural gas hydrates. Ph. D. Dis., Univ. of
496 Massachusetts .

497 Farrell, W.M., Delory, G.T., Atreya, S.K., 2006. Martian dust storms as a
498 possible sink of atmospheric methane. Geophysical research letters 33.

499 Fonti, S., Marzo, G.A., 2010. Mapping the methane on Mars. Astronomy &
500 Astrophysics 512, A51.

501 Forget, F., Hourdin, F., Fournier, R., Hourdin, C., Talagrand, O., Collins,
502 M., Lewis, S.R., Read, P.L., Huot, J.P., 1999. Improved general circula-
503 tion models of the Martian atmosphere from the surface to above 80 km.
504 Journal of Geophysical Research: Planets 104, 24155–24175.

505 Formisano, V., Atreya, S., Encrenaz, T., Ignatiev, N., Giuranna, M., 2004.
506 Detection of methane in the atmosphere of Mars. Science 306, 1758–1761.

507 Gainey, S.R., Elwood Madden, M.E., 2012. Kinetics of methane clathrate

formation and dissociation under Mars relevant conditions. Icarus 218, 513–524.

Geminale, A., Formisano, V., Giuranna, M., 2008. Methane in Martian atmosphere: Average spatial, diurnal, and seasonal behaviour. Planetary and Space Science 56, 1194–1203.

Geminale, A., Formisano, V., Sindoni, G., 2011. Mapping methane in Martian atmosphere with PFS-MEX data. Planetary and Space Science 59, 137–148.

Gillen, E., Rimmer, P.B., Catling, D.C., 2020. Statistical analysis of curiosity data shows no evidence for a strong seasonal cycle of martian methane. Icarus 336, 113407.

Giuranna, M., Viscardy, S., Daerden, F., Neary, L., Etiope, G., Oehler, D., Formisano, V., Aronica, A., Wolkenberg, P., Aoki, S., et al., 2019. Independent confirmation of a methane spike on Mars and a source region east of Gale Crater. Nature Geoscience 12, 326.

Gough, R.V., Tolbert, M.A., McKay, C.P., Toon, O.B., 2010. Methane adsorption on a Martian soil analog: An abiogenic explanation for methane variability in the Martian atmosphere. Icarus 207, 165–174.

Haberle, R.M., Clancy, R.T., Forget, F., Smith, M.D., Zurek, R.W., 2017. The atmosphere and climate of Mars. Cambridge University Press.

Hahn, B., McLennan, S., Klein, E., 2011. Martian surface heat production and crustal heat flow from Mars Odyssey Gamma-Ray spectrometry. Geophysical Research Letters 38.

Herri, J.M., Chassefière, E., 2012. Carbon dioxide, argon, nitrogen and methane clathrate hydrates: Thermodynamic modelling, investigation of their stability in Martian atmospheric conditions and variability of methane trapping. Planetary and Space Science 73, 376–386.

Holder, G.D., Corbin, G., Papadopoulos, K.D., 1980. Thermodynamic and molecular properties of gas hydrates from mixtures containing methane, argon, and krypton. Industrial & Engineering Chemistry Fundamentals 19, 282–286.

Holmes, J.A., Lewis, S.R., Patel, M.R., 2015. Analysing the consistency of martian methane observations by investigation of global methane transport. Icarus 257, 23–32.

Jensen, S.J.K., Skibsted, J., Jakobsen, H.J., ten Kate, I.L., Gunnlaugsson, H.P., Merrison, J.P., Finster, K., Bak, E., Iversen, J.J., Kondrup, J.C., Nørnberg, P., 2014. A sink for methane on Mars? The answer is blowing in the wind. Icarus 236, 24–27.

Jhaveri, J., Robinson, D.B., 1965. Hydrates in the methane-nitrogen system. The Canadian Journal of Chemical Engineering 43, 75–78.

Keppler, F., Vigano, I., McLeod, A., Ott, U., Früchtl, M., Röckmann, T., 2012. Ultraviolet-radiation-induced methane emissions from meteorites and the Martian atmosphere. Nature 486, 93.

Korablev, O., Vandaele, A.C., Montmessin, F., Fedorova, A.A., Trokhimovskiy, A., Forget, F., Lefèvre, F., Daerden, F., Thomas, I.R., Trompet,

L., et al., 2019. No detection of methane on Mars from early ExoMars Trace Gas Orbiter observations. Nature 568, 517.

Krasnopolsky, V.A., Maillard, J.P., Owen, T.C., 2004. Detection of methane in the martian atmosphere: evidence for life? Icarus 172, 537–547.

Kress, M.E., McKay, C.P., 2004. Formation of methane in comet impacts: implications for Earth, Mars, and Titan. Icarus 168, 475–483.

Kuhs, W.F., Klapproth, A., Gotthardt, F., Techmer, K., Heinrichs, T., 2000. The formation of meso-and macroporous gas hydrates. Geophysical research letters 27, 2929–2932.

Larson, S.D., 1955. Phase studies of the two-component carbon dioxide-water system, involving the carbon dioxide hydrate. Ph. D. Thesis, Univ. of Michigan .

Lasue, J., Quesnel, Y., Langlais, B., Chassefière, E., 2015. Methane storage capacity of the early Martian cryosphere. Icarus 260, 205–214.

Lefèvre, F., Forget, F., 2009. Observed variations of methane on Mars unexplained by known atmospheric chemistry and physics. Nature 460, 720.

Lipenkov, V.Y., Istomin, V., 2001. On the stability of air clathrate-hydrate crystals in subglacial Lake Vostok, Antarctica. Materialy Glyatsiol. Issled 91, 2001.

Makogon, T.Y., Sloan, E.D.J., 1994. Phase equilibrium for methane hydrate from 190 to 262 K. Journal of Chemical and Engineering Data 39, 351–353.

574 Marshall, D.R., Saito, S., Kobayashi, R., 1964. Hydrates at high pressures:
575 Part I. Methane-water, argon-water, and nitrogen-water systems. AIChE
576 Journal 10, 202–205.

577 Max, M., Johnson, A., Clifford, S., 2011. Methane hydrate on Mars: a
578 resource-rich stepping stone to the outer planets, in: Proceedings of the
579 7th International Conference on Gas Hydrates (ICGH 2011), Edinburgh,
580 Scotland.

581 McKoy, V., Sinanoğlu, O., 1963. Theory of dissociation pressures of some
582 gas hydrates. The Journal of Chemical Physics 38, 2946–2956.

583 Mellon, M.T., Feldman, W.C., Prettyman, T.H., 2004. The presence and
584 stability of ground ice in the southern hemisphere of Mars. Icarus 169,
585 324–340.

586 Mellon, M.T., Jakosky, B.M., 1993. Geographic variations in the thermal and
587 diffusive stability of ground ice on Mars. Journal of Geophysical Research:
588 Planets 98, 3345–3364.

589 Miller, S.L., 1961. The occurrence of gas hydrates in the solar system. Pro-
590 ceedings of the National Academy of Sciences 47, 1798–1808.

591 Miller, S.L., Smythe, W.D., 1970. Carbon dioxide clathrate in the Martian
592 ice cap. Science 170, 531–533.

593 Millour, E., Forget, F., Spiga, A., Navarro, T., Madeleine, J.B., Montabone,
594 L., Pottier, A., Lefevre, F., Montmessin, F., Chaufray, J.Y., et al., 2015.
595 The Mars Climate Database (MCD version 5.2). EPSC Abstracts 10, 438.

Mohammadi, A.H., Richon, D., 2010. Ice–clathrate hydrate–gas phase equilibria for air, oxygen, nitrogen, carbon monoxide, methane, or ethane + water system. Industrial & Engineering Chemistry Research 49, 3976–3979.

Mohammadi, A.H., Richon, D., 2011. Ice–clathrate hydrate–gas phase equilibria for argon + water and carbon dioxide + water systems. Industrial & Engineering Chemistry Research 50, 11452–11454.

Mousis, O., Chassefière, E., Lasue, J., Chevrier, V., Elwood Madden, M.E., Lakhlifi, A., Lunine, J.I., Montmessin, F., Picaud, S., Schmidt, F., et al., 2013. Volatile trapping in Martian clathrates. Space Science Reviews 174, 213–250.

Mousis, O., Simon, J.M., Bellat, J.P., Schmidt, F., Bouley, S., Chassefière, E., Sautter, V., Quesnel, Y., Picaud, S., Lectez, S., 2016. Martian zeolites as a source of atmospheric methane. Icarus 278, 1–6.

Mumma, M.J., Villanueva, G.L., Novak, R.E., Hewagama, T., Bonev, B.P., DiSanti, M.A., Mandell, A.M., Smith, M.D., 2009. Strong release of methane on Mars in northern summer 2003. Science 323, 1041–1045.

Ng, H.J., Robinson, D.B., 1985. Hydrate formation in systems containing methane, ethane, propane, carbon dioxide or hydrogen sulfide in the presence of methanol. Fluid Phase Equilibria 21, 145–155.

Oze, C., Sharma, M., 2005. Have olivine, will gas: Serpentinization and the abiogenic production of methane on Mars. Geophysical Research Letters 32.

Parro, L.M., Jiménez-Díaz, A., Mansilla, F., Ruiz, J., 2017. Present-day heat flow model of Mars. Scientific Reports 7.

Prieto-Ballesteros, O., Kargel, J.S., Fairén, A.G., Fernández-Remolar, D.C., Dohm, J.M., Amils, R., 2006. Interglacial clathrate destabilization on Mars: Possible contributing source of its atmospheric methane. Geology 34, 149–152.

Putzig, N.E., Mellon, M.T., 2007. Apparent thermal inertia and the surface heterogeneity of Mars. Icarus 191, 68–94.

Robinson, D.B., Hutton, J.B., et al., 1967. Hydrate formation in systems containing methane, hydrogen sulphide and carbon dioxide. Journal of Canadian Petroleum Technology 6, 6–9.

Root, M.J., Elwood Madden, M.E., 2012. Potential effects of obliquity change on gas hydrate stability zones on Mars. Icarus 218, 534–544.

Schorghofer, N., Aharonson, O., 2005. Stability and exchange of subsurface ice on Mars. Journal of Geophysical Research: Planets 110.

Schuerger, A.C., Ulrich, R., Berry, B.J., Nicholson, W.L., 2013. Growth of *Serratia liquefaciens* under 7 mbar, 0°C, and CO_2-enriched anoxic atmospheres. Astrobiology 13, 115–131.

Sloan, E.D., Koh, C.A., 2007. Clathrate hydrates of natural gases. 3rd ed., CRC press, Boca Raton.

Strobel, T.A., Koh, C.A., Sloan, E.D., 2009. Thermodynamic predictions

of various tetrahydrofuran and hydrogen clathrate hydrates. Fluid Phase Equilibria 280, 61–67.

Takenouchi, S., Kennedy, G.C., 1965. Dissociation pressures of the phase $CO_2 \cdot$ 5 3/4 H_2O. The Journal of geology 73, 383–390.

Thomas, C., Mousis, O., Picaud, S., Ballenegger, V., 2009. Variability of the methane trapping in martian subsurface clathrate hydrates. Planetary and Space Science 57, 42–47.

Villanueva, G.L., Mumma, M.J., Novak, R.E., Radeva, Y.L., Käufl, H.U., Smette, A., Tokunaga, A., Khayat, A., Encrenaz, T., Hartogh, P., 2013. A sensitive search for organics (CH_4, CH_3OH, H_2CO, C_2H_6, C_2H_2, C_2H_4), hydroperoxyl (HO_2), nitrogen compounds (N_2O, NH_3, HCN) and chlorine species (HCl, CH_3Cl) on Mars using ground-based high-resolution infrared spectroscopy. Icarus 223, 11–27.

van der Waals, J., Platteeuw, J., 1959. Clathrate solutions. Advances in Chemical Physics, Volume 2 , 1–57.

Webster, C.R., Mahaffy, P.R., Atreya, S.K., Flesch, G.J., Mischna, M.A., Meslin, P.Y., Farley, K.A., Conrad, P.G., Christensen, L.E., Pavlov, A.A., et al., 2015. Mars methane detection and variability at Gale crater. Science 347, 415–417.

Webster, C.R., Mahaffy, P.R., Atreya, S.K., Moores, J.E., Flesch, G.J., Malespin, C., McKay, C.P., Martinez, G., Smith, C.L., Martin-Torres, J., et al., 2018. Background levels of methane in Mars atmosphere show strong seasonal variations. Science 360, 1093–1096.

663 Webster, C.R., Mahaffy, P.R., Atreya, S.K., Flesch, G.J., Farley, K.A., et al.,
664 2013. Low upper limit to methane abundance on Mars. Science , 1242902.

665 Weiss, B.P., Yung, Y.L., Nealson, K.H., 2000. Atmospheric energy for sub-
666 surface life on Mars? Proceedings of the National Academy of Sciences
667 97, 1395–1399.

668 Yasuda, K., Ohmura, R., 2008. Phase equilibrium for clathrate hydrates
669 formed with methane, ethane, propane, or carbon dioxide at temperatures
670 below the freezing point of water. Journal of Chemical & Engineering Data
671 53, 2182–2188.

672 Zahnle, K., 2015. Play it again, SAM. Science 347, 370–371.

673 Zahnle, K., Freedman, R.S., Catling, D.C., 2011. Is there methane on Mars?
674 Icarus 212, 493–503.